On thermoelectric and pyroelectric energy harvesting

Gael Sebald[1,3], Daniel Guyomar[1] and Amen Agbossou[2]

[1] Université de Lyon, INSA de Lyon, LGEF, 8 rue de la physique, 69621 Villeurbanne cedex, France

[2] Université de Savoie, LOCIE—CNRS FRE 3220, Campus scientifique—Savoie Technolac, 73376 Le Bourget du Lac Cedex, France

E-mail: gael.sebald@insa-lyon.fr

Abstract

This paper deals with small-power energy harvesting from heat. It can be achieved using both thermoelectric and pyroelectric effects. In the first case, temperature gradients are necessary. The main difficulty of thermoelectric energy harvesting is imposing a large temperature gradient. This requires huge heat flows because of the limited surface heat exchanges and the large heat conductivity of thermoelectric materials. This results in a drastic decrease of power and the efficiency of conversion. In case of pyroelectric energy harvesting, a time varying temperature is necessary. Although such a temperature time profile is hard to find, the overall optimization is easier than the thermoelectric strategy. Indeed, it depends much less on heat exchange between the sample and the outer medium, than on heat capacity that dimensions optimization may easily compensate. As a consequence, it is shown that the efficiency and output power may be much larger using pyroelectric energy harvesting than thermoelectric methods. For instance, using a limited temperature gradient due to the limited heat exchange, a maximum efficiency of 1.7% of Carnot efficiency can be expected using a thermoelectric module. On the contrary, a pyroelectric device may reach an efficiency up to 50% of Carnot efficiency. Finally, an illustration shows an estimation of the output power that could be expected from natural time variations of temperature of a wearable device. Power peaks up to 0.2 mW cm^{-3} were found and a mean power of 1 μW cm^{-3} on average was determined within 24 h testing.

Introduction

Constant advances in electronics push past boundaries of integration and functional density towards completely autonomous microchips embedding their own energy source. A research effort on higher energy-density batteries is important, but for long lasting or harsh environment applications such a solution lacks reliability and has high maintenance costs. One of the most challenging ways to self-power devices is the development of systems that recycle ambient energy and continually replenish the energy consumed by the system. Some possible ambient energy sources are for instance thermal energy, light energy or mechanical energy. Harvesting energy from such renewable sources has stimulated important research efforts in recent years. Several devices from the millimeter scale down to the microscale have been presented, with average powers in the 10 μW–10 mW range [1].

Energy harvesting systems have attracted different research specialties and have been of increasing interest during the last 10 years. Significant effort concentrated on vibration energy harvesting has led to some of the most promising solutions for autonomous self-power and wireless sensors networks [2, 3]. Apart from centimeter size devices (in the tens or hundred of milliwatt range), researchers from Microsystems Devices (Micro Electro Mechanical Systems or MEMS) strongly believe in energy harvesting development. Techniques used for energy harvesting are numerous:

- Photovoltaic—solar energy is directly converted into electrical energy using polarized solar cells (semiconductor devices).

---

[3] Author to whom any correspondence should be addressed.

- Mechanical (vibrations):
  * Electrostatic method—a relative movement between electrically isolated charged capacitor planes is utilized. The work against the electrostatic force between the plates provides the harvested energy [4].
  * Electromagnetic method—an electromagnetic induction arising form the relative motion (rotative or linear) between a magnetic flux and a conductor is used [5].
  * Piezoelectric method—active materials are employed to generate the energy when mechanically stressed [6].
- Thermal—thermal energy (temperature gradient) is converted into electrical energy using e.g. Seebeck's effect [7].
- Thermal—thermal energy (temperature variation) is converted via the pyroelectric effect.

Innovative solutions are now proposed commercially and—in order to give one example among others—some applications may be found in the Enocean® product description. The output powers and operating conditions are numerous depending on the size constraints and available energy sources (illumination level, vibration amplitudes and frequencies, external temperature gradients or variation). Any of these techniques may be the best solution for a given self-powered device, and within this paper, we will not plot the advantages and drawbacks of each technique since these are complementary. We focus here on the last two energy harvesting strategies. Heat could be the only energy source for indoor and static (without vibration) devices.

Thermoelectric modules are the main way for energy harvesting from temperature. It is now possible to find commercial thermoelectric generators from μW to kW in electric output energy. These are based on temperature gradients leading to heat flow through the thermoelectric generator and a small percentage of the heat flow is converted to electric energy. Material properties are the key parameter for improving both the output power (the increase of the thermal heat flow thus making it difficult to keep the temperature gradient) and the efficiency (improving the Seebeck coefficient and figure of merit).

Pyroelectric materials may be used for thermal energy to electric energy conversion. Contrary to the thermoelectric generator, pyroelectric materials do not need a temperature gradient (spatial gradient), but temporal temperature changes. Application targets are then quite different, such as small-scale microgenerators with dimensions smaller than the temperature spatial fluctuation. It is also possible to transform a temperature gradient into a temperature variable in time using a caloric fluid pumping between hot and cold reservoirs.

Both energy harvesting strategies are of great interest for microgenerators self-powering sensor networks, and we aim in this paper to plot the main differences between the two strategies. Although using different temperature characteristics (thermal gradient for thermoelectric and time varying temperature for pyroelectric), it is still possible to transform a time variation into a space gradient to use only

thermoelectric technology. However, this may not be the most effective way of energy harvesting. Furthermore, the performances of pyroelectric energy harvesting may be larger than thermoelectric ones in some cases.

The work presented in the paper deals with the main differences between thermoelectric and pyroelectric energy harvesting, and the drawbacks of both strategies. Finally, the influence of limited surface heat exchange between the outer medium and active material is investigated. The paper is structured as follows. Section 1 is devoted to the pyroelectric energy harvesting case and numerical simulations illustrating the power per unit volume that could be expected with a standard energy conversion (resistance connected to the pyroelectric material). To do so, pyroelectric properties from bibliographic data are used for a energy harvesting estimation. Within the same section, a presentation of nonlinear pyroelectric energy harvesting is presented, including a quick materials comparison. In section 2, thermoelectric energy harvesting is presented. It is shown that the difficulty of maintaining a large temperature gradient results in a limited performance. Finally, a discussion on both strategies is proposed and an illustration of naturally varying temperature concludes the work.

1. Pyroelectric energy harvesting

1.1. Using linear pyroelectric properties

This section aims at showing the capabilities of pyroelectric materials to harvest energy when subjected to cyclic temperature variations. We consider here idealized pyroelectric materials exhibiting no losses and purely linear properties. The development of the pyroelectric equations was presented in a previous paper [8]. We add here the problem of limited heat exchange on the outer surface of the pyroelement.

Neglecting dielectric losses, the pyroelectric equations are:

$$\dot{D} = \varepsilon \dot{E} + p\dot{\theta} \qquad (1)$$

$$\dot{S} = p\dot{E} + c\dot{\theta}/\theta \qquad (2)$$

where D, E, θ and S are the electric induction, electric field, temperature and entropy respectively. The pyroelement coefficients ε, p and c are dielectric permittivity, pyroelectric coefficient and heat capacity respectively.

Based on Newton diffusion, the equation coupling the external variables to the pyroelement ones are

$$Q = -\frac{h}{e}(\theta - \theta_{\text{ext}}) \qquad (3)$$

$$E = -\rho \dot{D} \qquad (4)$$

where Q and θ_{ext} are the exchanged heat per unit of volume and the external temperature respectively on one hand, and h, e, and ρ are the surface heat exchange, sample thickness and resistivity connected to the pyroelement respectively. Dotted variables denote time derivatives.

We consider here an electrical loading of the pyroelectric element, which simulates the utilization of the generated power. When the electrical loading is purely resistive, the
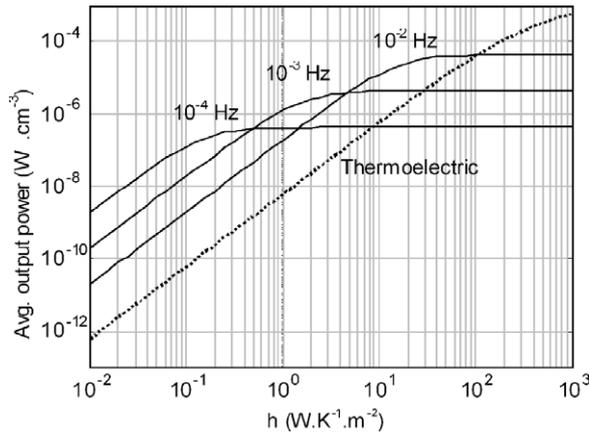
Figure 1. Average output power on adapted resistance for pyroelectric and thermoelectric energy harvesting. For both cases the same temperature amplitude (20 °C peak–peak) and same thickness (100 μm) are considered in the simulations.

electric field and electric induction exhibit a $\pi/2$ phase shift. As a consequence, the average output electrical power is non-zero. In addition, the electrical loading is expressed as a resistivity in order to obtain simulations that give the output power per unit volume without loss of generality. In the simulations, the value of the resistivity is chosen so that the output power is maximized.

Furthermore, we consider here a single disk-shape plate of pyroelectric material. The thickness is assumed to be much smaller that the diameter of the plate. Due to the dimension ratio, we assume a uniform temperature of the element (heat conductivity × thickness is considered much higher than surface heat exchange). The results presented here do not depend on element dimensions, since they are expressed per unit volume. In the following, the results are presented as a function of the heat exchange. It depends mainly on the structural design, such as radiators allowing an artificially increased surface area or fans allowing a much larger heat exchange. In addition, other parameters may change this parameter, such as the roughness of the surface, Finally, it is possible to work with other fluids such as oil or water that largely increase the heat exchange.

In figure 1 three curves are shown for pyroelectric energy harvesting at different frequencies (solid lines). In the simulation, thickness was chosen to be 100 μm. Material properties and simulation parameters are detailed in table 1. It corresponds to the properties of 0.75Pb(Mg$_{1/3}$Nb$_{2/3}$)O$_3$–0.25PbTiO$_3$ ceramic [9]. The output power per unit volume is calculated for a 20 °C peak-to-peak temperature variation, and for three different frequencies of temperature variation (solid lines in the figure). For each case, the power is plotted as a function of the heat exchange coefficient.

For a given frequency, increasing the heat exchange results in an increase of the harvested power. On the contrary, when reaching the high heat exchange region, the pyroelement temperature is always at equilibrium with the external temperature. In addition, increasing the frequency also results in an increase of output power. For a given

Table 1. Parameters used for simulations of pyroelectric energy harvesting. The material is a ceramic of 0.75Pb(Mg$_{1/3}$Nb$_{2/3}$)O$_3$–0.25PbTiO$_3$.

Parameter	Value
Pyroelectric coefficient p	746 μC m^{-2} K^{-1}
Dielectric permittivity ε	2100 ε_0
Heat capacity c	2.5×10^6 J m^{-3} K^{-1}
Temperature amplitude	20 °C peak–peak

temperature variation frequency, there exist a threshold for the heat exchange coefficient that is necessary to maximize the output power.

1.2. Towards giant energy harvesting

The results presented in section 1.1 correspond to low output power, as an example, using a temperature variation of 20 °C peak-to-peak at 10^{-2} Hz, and considering a heat exchange of 10 W m^{-2} K^{-1} (forced convection with air), we obtain an output power of 13.4 μW cm^{-3}. This corresponds to a real temperature variation of 5.4 K due to the limited heat exchange.

In this section we aim to show that the previously presented result corresponds to a minimum of power that can be harvested using pyroelectric coupling. Using nonlinear materials, it is possible to greatly increase these results as explained below. After the presentation of the energy harvesting principle the output power estimation is presented from bibliographic data.

The associated techniques lie on performing thermodynamic cycles in the polarization–electric field plane (P–E plane) associated with a cycle in the entropy–temperature plane (Γ–θ plane). These are named Stirling, Ericsson [18–20] or Olsen cycles [21–24]. In such a way, it is possible to greatly enhance the global electrothermal coupling of the materials. The basic idea is to work in the vicinity of a phase transition where the polarization is greatly affected by temperature variations.

The thermodynamic cycle is obtained by continuously applying an electric field to the sample from 0 to a maximum value synchronously with the temperature variation with a $\pi/2$ phase shift. When the temperature decreases the voltage is kept at zero. On reaching the minimum temperature the voltage is rapidly increased to its maximum value. Then the voltage is kept high until the temperature increases to its maximum value. Finally the voltage is decreased to zero. This induces a phase shift between the electric charge and the voltage thus leading to a non-zero average output electrical power. More details on this process are given in the bibliographic data [18–24].

In table 2 are shown the expected output power for the same temperature solicitations as in section 1.1 for different materials; linear and nonlinear. We selected representative materials for the demonstration (not exhaustive). For nonlinear materials, we present the electrocaloric activity and the associated effective expected output power for the same conditions as the previous simulation. This power is estimated using the electrocaloric activity from an equivalence presented

Table 2. Properties of linear and nonlinear pyroelectric materials, and the expected output power for an external temperature variation of 20 °C peak–peak at 10^{-2} Hz, with $h = 10$ W m^{-2} K^{-1}, and a thickness of 100 μm. (SC = single crystal, C = ceramic, TF = thin film, P = polymer). For the linear materials, the energy harvesting is performed using an adapted load resistance connected directly on the sample. For nonlinear materials, an Ericsson cycle is considered where the maximum applied electric field is indicated in the fourth column.

Linear materials	Shape	p (μC m^{-2} K^{-1})	$\varepsilon_{33}^{\theta}$ (ε_0)	c_E ($\times 10^6$ J m^{-3} K^{-1})	P_{out} (μW cm^{-3})	Ref.
111 PMN–0.25PT single crystals	SC	1300–1790	961–1100	2.5	100–169	[9, 10]
PZT	C	533	1116	2.5	12.9	[11]
PMN–0.25PT ceramic	C	746	2100	2.5	13.4	[12]
PVDF	P	33	9	1.8	6.12	[13]

Nonlinear materials	Shape	Q_{ECE} (J cm^{-3})	Applied electric amplitude (kV mm^{-1})	θ_{cold} (°C)	P_{out} (μW cm^{-3})	Ref.
0.95PbSc$_{0.5}$Ta$_{0.5}$O$_3$–0.05PbSc$_{0.5}$Sb$_{0.5}$O$_3$	C	4.2	2.5	−5	1570	[14]
0.90Pb(Mg$_{1/3}$Nb$_{2/3}$)O$_3$–0.10PbTiO$_3$ ceramic	C	1.4	3.5	30	500	[20]
⟨110⟩ 0.955 Pb(Zn$_{1/3}$Nb$_{2/3}$)O$_3$–0.045PbTiO$_3$ single crystal	SC	No measure	2	90	750	[19]
0.90Pb(Mg$_{1/3}$Nb$_{2/3}$)O$_3$–0.10PbTiO$_3$ thin film	TF	15	90	75	4320	[15]
PZST75/20/5	C	9.8	3	160	2240	[16]
PbZr$_{0.95}$Ti$_{0.05}$O$_3$ thin film	TF	30	78	220	5960	[17]

in [20]. Indeed, energy harvesting can be calculated from the electrocaloric effect using

$$W_e = -\eta_{Carnot} Q_{ECE} \qquad (5)$$

where W_e, η_{Carnot} and Q_{ECE} are the harvested energy per cycle, the Carnot ideal cycle efficiency and the electrocaloric heat respectively.

Then power is simply obtained by multiplying this energy by the working frequency.

The electrocaloric effect is the ability to change the temperature (in adiabatic case) or the entropy (in isothermal case) upon the application of an electric field. The necessary value of the electric field for Ericsson cycles is also indicated. It is noticeable that power is increased by a factor of 10–600 compared to linear pyroelectric energy harvesting. One can understand the magnification of power by considering an effective electrothermal coupling that becomes very large in the vicinity of phase transitions. The better known result is the outstanding electrocaloric activity. Here we utilize the inverse effect leading to outstanding energy harvesting.

This should be balanced with the fact that we still need the development of electronics which are able to apply an electric field and be fully reversible. On the other hand, the working temperature range is limited to the phase transition vicinity. For a given expected temperature variation, it is then necessary to choose an appropriate material, whereas in the case of a purely linear pyroelectric material, a large range of working temperatures is possible. Nevertheless, this shows that the previously presented comparison between linear pyroelectric energy harvesting may be considered as a minimum of achievable energy harvesting from pyroelectric coupling.

2. Thermoelectric energy harvesting

Thermoelectric devices can convert a heat flow into an electric power. Known for almost two centuries, such a class of generators had not found many applications except for aerospace [25] (for example, energy sources of deep space probes whose heating source is a radioisotope). However, recent developments of microgenerators for portable and pervasive computing devices make this solution of interest for self-powering devices. Performance of a thermoelectric module can be estimated via the Ioffe figure of merit (Z); although now, we prefer to talk about the ZT figure of merit by multiplying Ioffe's figure by the temperature of the hot junction T.

However, it was recently demonstrated that this figure of merit does not really express the performance of a thermoelectric generator when considering the limited heat exchange on the outer surfaces of the thermoelectric module [26]. Apart from Seebeck effect and thermoelectric generator design, parameters such as the heat loss of the Joule and Peltier effects caused by the electric current largely affect the performance. This is due to the fact that a limited heat exchange on the outer surfaces results in a decrease of the actual temperature gradient and thus makes the Joule and Peltier effect much more important in the performance loss than what could be expected from the single figure of merit.

We aim in this paper to show realistic output powers of a thermoelectric module when considering the limited heat exchange on the outer surfaces. Indeed several publications show a very large output power using thermoelectric modules (>100 W), but they require a forced heat exchange between the two surfaces of the module, for example using pumping fluids between the hot and cold reservoirs [27–29]. This latter point is unlikely to fulfil volume constraints where adding pump, fluids and heat exchangers results in bulky and heavy structures, even if the active material can be compact.

On the contrary, attempts to convert human body heat into electricity usually state a global temperature gradient of about 10–20 °C (between the body temperature and the outer

Table 3. Parameters used in the simulation of thermoelectric energy harvesting.

Parameter	Value
Seebeck coefficient α	2.2×10^{-4} V K^{-1}
Heat conductivity γ	1.5 W m^{-1} K^{-1}
Internal resistivity ρ	10^{-5} Ω m^{-1}
Thickness e	10^{-4} m
ZT ($\theta_{\text{hot}} = 320$ K)	1

medium). However, due to limited heat exchange, the actual gradients hardly reach a few degrees, resulting in a very limited output power [30]. Although a large figure of merit may be obtained from advanced materials, the subsequent expected performances cannot be reached due to the impossibility of ensuring a temperature gradient as large as the external one.

In order to illustrate this point, we simulate here the power conversion of a thermoelectric module whose properties are given in table 3. The calculation is done using equations from [26] on adapted resistance. The thermoelectric module output power as a function of electrical loading reaches a maximum when the electrical loading equals the internal resistance of the thermoelectric module, and this value is called the adapted resistance.

The first step is to calculate the actual temperature gradient of the element that differs from external temperature gradient. In a second step, the output power can be calculated from temperature gradient on the thermoelectric module. The electrical loading simulates the utilization of the output power. The temperature gradient is calculated using

$$a\Delta\theta^3 + b\Delta\theta + c\Delta\theta_{\text{ext}} = 0 \qquad (6)$$

where $a = \frac{\alpha^4}{8\rho^2 e^2}$, $b = \frac{\gamma\alpha^2}{\rho^2 e}\theta_{\text{mean}} + \frac{2\gamma h}{e} + h^2$, $c = h^2$; $\Delta\theta_{\text{ext}}$, ρ, γ, e, and h are external temperature difference, electrical conductivity, thermal conductivity, thickness and surface heat exchange coefficient respectively.

Then, output power per unit volume is obtained using

$$P_{\text{vol}} = \frac{\alpha^2 \Delta\theta^2}{2\rho e^2}. \qquad (7)$$

The output power on an adapted resistor is plotted against the surface heat exchange for a given 20 °C temperature difference between the hot and cold reservoirs. We chose the same thickness as for pyroelectric case.

The results are shown in figure 2. As mentioned before, the actual temperature gradient is much lower than the outer temperature difference. Even for an excessive surface heat exchange coefficient of 1000 W m^{-2} K^{-1}, we are still lower than the external temperature gradient. As a consequence, for limited heat exchange, there is a big difference between the external and module gradients. For a realistic heat exchange coefficient in the range 1–10 W m^{-2} K^{-1}, the actual temperature gradient is in the range 4.4×10^{-4}–4.4×10^{-3} K and the output power falls between 2.4×10^{-8} and 2.4×10^{-6} W cm^{-3}. As a consequence, a heat exchanger increasing exchange area, coupled with forced air convection or a fluid, is necessary in order to ensure a higher temperature gradient.
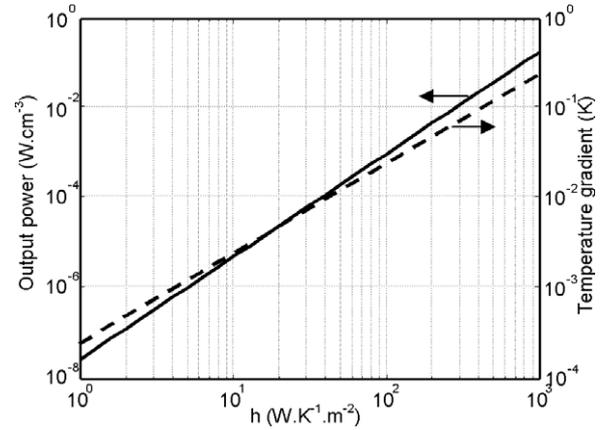
Figure 2. Thermoelectric actual gradient and output power for an external temperature gradient of 20 °C as a function of surface heat exchange. Output power on the left scale (solid line) and temperature gradient on the right scale (dotted line).

3. Discussion

As stated before, we aim in this paper to compare energy harvesting using pyroelectricity or thermoelectricity. Both power simulations are presented in figure 1. It is shown that the overall output power using a linear pyroelectric material may be superior to that of a good thermoelectric material (by a factor of 10). Furthermore, as explained in section 1.2, using nonlinear pyroelectric materials can result in a further gain of 10–100 on the performance. The explanation of this observation is two-fold:

(i) From heat exchange considerations, the pyroelectric material is expected to follow the outer temperature variation closely. The key parameter is the surface heat exchange combined with the heat capacity. The time constant of heat exchange is

$$\tau = \frac{ec}{h}, \qquad (8)$$

where e, c and h are thickness, heat capacity and surface heat exchange respectively. Energy harvesting is optimal when the temperature period is larger that the thermal time constant. On the contrary, thermoelectric energy harvesting requires ensuring the maximum temperature gradient between the hot and cold surface, and this capability depends on the surface heat exchange and heat conductivity. Materials exhibiting a large ZT value usually also exhibit quite large heat conductivities. As a consequence, for a large temperature gradient a huge surface heat exchange is required. Neglecting Joule and Peltier influence on the temperature gradient, and assuming the same surface heat exchange for the two surfaces, the temperature gradient is expressed as

$$\Delta\theta = \frac{\Delta\theta_{\text{ext}}}{1 + 2\gamma/eh}. \qquad (9)$$

The temperature gradient does not depend on the heat capacity unlike the pyroelectric case; this is why optimization for limited heat exchange is very different. In

the pyroelectric case, we face the optimization of periodic heat transfer whereas in the thermoelectric case, we face the optimization of the heat flow.

(ii) Another way to plot the fundamental difference between thermoelectric and pyroelectric energy harvesting is to consider the efficiency related to the efficiency of an ideal Carnot cycle. For a 20 °C peak–peak temperature variation or gradient around room temperature, the Carnot efficiency is 6.7%. In the case of pyroelectric energy harvesting, it is possible to reach a global efficiency of 5%–10% of Carnot efficiency (thus leading to a maximum global efficiency of 0.67%). In the case of thermoelectric energy harvesting, it is limited to similar values provided that the modules gradient is the same as the external one. Compared to thermoelectric energy harvesting—where efficiency is limited by material properties—the efficiency for pyroelectric materials may tend to the Carnot's efficiency. The thermoelectric conversion efficiency may be expressed as [31, 32]

$$\eta = \frac{\theta_h - \theta_c}{\theta_h} \frac{\sqrt{ZT + 1} - 1}{\sqrt{ZT + 1} + \theta_h/\theta_c}. \qquad (10)$$

For the best thermoelectric materials, the figure of merit ZT reaches 1 around room temperature with Bi_2Te_3 materials, for example [33]. As a result, the best efficiency reaches 17% of the Carnot efficiency (considering low temperatures differences in order to maximize the efficiency). In order to get 50% of the Carnot efficiency, one should find a material having a figure of merit of 9, which is ten times higher than the best known thermoelectric materials. Furthermore, in equation (9), the temperatures are temperatures of the thermoelectric module. When considering the hot and cold reservoir temperatures, the actual Carnot efficiency is much larger, and this relative efficiency decreases by the ratio between the expected temperature gradient and the actual temperature gradient. For instance, when considering an efficiency related to the Carnot efficiency of 17% (using a material with $ZT = 1$), if the actual temperature gradient of the module is ten times lower than the external one, then the efficiency related to Carnot efficiency will be as low as 1.7%.

Nonlinear pyroelectric materials may, in theory, lead to much higher efficiency by using, for example, a stack of elements working with different temperature variations always adapted to get the highest efficiency per layer. The theoretical efficiency is that of Carnot. For a single unit, efficiencies up to 50% may be expected by the use of thin films [20].

However these advantages for pyroelectric energy conversion must be counterbalanced with the need for temperature time variations. Natural temperature variations are quite unusual in the practical case whereas it is easy to find temperature space gradients. It is however possible to create such time variations from spatial gradients using, for example, a cyclic pumping unit as demonstrated theoretically by Sklar [34]. The pump power consumption may be as little as 2% of the total harvested energy.

It is also possible to find natural temperature variations in portable devices, for example a piece of the fabric of a coat and going from inside to outside several times per day. In
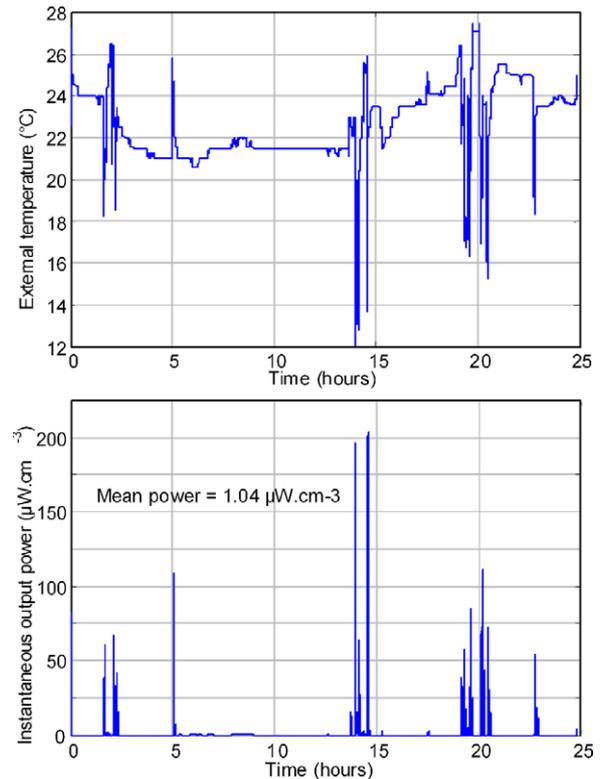

Figure 3. Experimental natural temperature variations recorded during 24 h (top) and estimation of energy harvesting using a pyroelectric material (properties of PMN–PT single crystal, first line of table 2).

(This figure is in colour only in the electronic version)

order to illustrate the latter point, we measured, within 24 h, the temperature of the outer side of a coat using a temperature recorder with a thermocouple probe (probe dimension is 2 mm diameter by 10 cm long). Here we aim at giving an example of the quantification of the output power that can be expected from a naturally varying temperature. In the experiment, only the temperature was recorded, and we calculate an output power by assuming that the same temperature profile is applied to a pyroelectric material. A coarse estimation of the possible harvested energy was calculated theoretically by considering a resistance connected to the pyroelectric material so that the time constant of the RC circuit is 30 s (the temperature spectrum is maximum around 3×10^{-2} Hz). The properties of the pyroelectric material are the same as those in table 1. Power peaks up to 0.2 mW cm^{-3} were found and a mean power of 1 μW cm^{-3} was determined within this 24 h testing (figure 3). Furthermore, the measurement probe was a cylinder of diameter 2 mm by 10 cm long. A much thinner structure would give faster and larger temperature variations. The obtained power is very small (sufficient only for powering a watch). This amount of energy is insufficient to power mobile devices or sensor networks unless the working time is much smaller than the waiting time (it could be unnecessary for a sensor to deliver its value continuously). However, further optimization of electronics power consumption is necessary so that this power generation meets mobile devices power requirements.

4. Conclusion

In this paper, we proposed a comparison between thermoelectric and pyroelectric energy harvesting. We aimed to point out the fundamental differences between the two strategies to develop microgenerators working from heat. Both are complementary since their optimization would be different. Although pyroelectric energy harvesting may seem to give little energy, it has a greater efficiency compared to the thermoelectric case and it is much easier to get it to work using limited surface heat exchanges. Thermoelectric materials are difficult to implement due to their typically large heat conductivities that drastically decrease the actual temperature gradient, and thus the efficiency and power. Pyroelectric materials do not suffer such a limitation and may work much closer to the Carnot efficiency.

Finally we showed a quick experiment of a naturally time varying temperature and its related energy harvesting estimation. This exhibited a mean power of 1 μW cm^{-3} with peaks above 0.2 mW cm^{-3}.

Acknowledgment

References

[1] Roundy S, Leland E S, Baker J, Carleton E, Reilly E, Lai E, Otis B, Rabaey J M, Sundararajan V and Wright P K 2005 Improving power output for vibration-based energy scavengers *IEEE Pervas. Comput.* **4** 28–36

[2] Roundy S, Wright P K and Rabaey J 2003 A study of low-level vibrations as a power source for wireless sensor nodes *Comput. Commun.* **26** 1131–44

[3] Guyomar D, Jayet Y, Petit L, Lefeuvre E, Monnier T, Richard C and Lallart M 2007 Synchronized switch harvesting applied to selfpowered smart systems: piezoactive microgenerators for autonomous wireless transmitters *Sensors Actuators* A **138** 151–60

[4] Peano F and Tambosso T 2005 Design and optimization of a MEMS electret-based capacitive energy scavenger *J. Microelectromech. Syst.* **14** 429–35

[5] Glynne-Jones P, Tudor MJ, Beeby SP and White NM 2004 An electromagnetic, vibration-powered generator for intelligent sensor systems *Sensors Actuators* A **110** 344–9

[6] Guyomar D, Badel A, Lefeuvre E and Richard C 2005 Toward energy harvesting using active materials and conversion improvement by nonlinear processing *IEEE Trans. Ultrason. Ferroelectr. Freq. Control* **52** 584–95

[7] DiSalvo F J 1999 Thermoelectric cooling and power generation *Science* **285** 703–6

[8] Sebald G, Lefeuvre E and Guyomar D 2008 Pyroelectric energy conversion: optimization principles *IEEE Trans. Ultrason. Ferroelectr. Freq. Control* **55** 538–51

[9] Sebald G, Seveyrat L, Guyomar D, Lebrun L, Guiffard B and Pruvost S 2006 Electrocaloric and pyroelectric properties of 0.75Pb(Mg$_{1/3}$Nb$_{2/3}$)O$_3$–0.25PbTiO$_3$ single crystals *J. Appl. Phys.* **100** 124112

[10] Davis M, Damjanovic D and Setter N 2004 Pyroelectric properties of $(1 − x)$Pb(Mg$_{1/3}$Nb$_{2/3}$)O$_3$–xPbTiO$_3$ and $(1 − x)$Pb(Zn$_{1/3}$Nb$_{2/3}$)O$_3$–xPbTiO$_3$ single crystals measured using a dynamic method *J. Appl. Phys.* **96** 2811–5

[11] Ng W Y, Ploss B, Chan H L W, Shin F G and Choy C L 2000 Pyroelectric properties of PZT/P(VDF-TrFE) 0–3 composites *ISAF 2000: Proc. 2000 12th IEEE Int. Symp. on Applications of Ferroelectrics* vol 2, pp 767–70

[12] Guyomar D, Sebald G, Guiffard B and Seveyrat L 2006 Ferroelectric electrocaloric conversion in 0.75(PbMg$_{1/3}$Nb$_{2/3}$O$_3$)–0.25(PbTiO$_3$) ceramics *J. Phys. D: Appl. Phys.* **39** 4491–6

[13] Lang S B and Muensit S 2006 Review of some lesser-known applications of piezoelectric and pyroelectric polymers *Appl. Phys.* A **25** 125–34

[14] Shebanov L and Borman K 1992 On lead–scandium tantalate solid solutions with high electrocaloric effect *Ferroelectrics* **127** 143–8

[15] Mischenko A S, Zhang Q, Whatmore R W, Scott J F and Mathur N D 2006 Giant electrocaloric effect in the thin film relaxor ferroelectric 0.9PbMg$_{1/3}$Nb$_{2/3}$O$_3$–0.1PbTiO$_3$ near room temperature *Appl. Phys. Lett.* **89** 242912

[16] Tuttle A and Payne D A 1981 The effects of microstructure on the electrocaloric properties of Pb (Zr, Sn, Ti) O$_3$ ceramics *Ferroelectrics* **37** 603

[17] Mischenko A S, Zhang Q, Scott J F, Whatmore R W and Mathur N D 2006 Giant electrocaloric effect in thin-film PbZr$_{0.95}$Ti$_{0.05}$O$_3$ *Science* **311** 1270–1

[18] Guyomar D, Pruvost S and Sebald G 2008 Energy harvesting based on FE–FE transition in ferroelectric single crystals *IEEE Trans. Ultrason. Ferroelectr. Freq. Control* **55** 279–85

[19] Khodayari A, Pruvost S, Sebald G and Guyomar D 2009 Non linear pyroelectric energy harvesting from relaxor single crystals *IEEE Trans. Ultrason. Ferroelectr. Freq. Control* **56** 693–9

[20] Sebald G, Pruvost S and Guyomar D 2008 Energy harvesting based on Ericsson pyroelectric cycles in relaxor ferroelectric ceramic *Smart Mater. Struct.* **17** 015012

[21] Olsen R B and Evans D 1983 Pyroelectric energy conversion: hysteresis loss and temperature sensitivity of a ferroelectric material *J. Appl. Phys.* **54** 5941–4

[22] Olsen R B, Bruno D A and Briscoe J M 1985 Pyroelectric conversion cycles *J. Appl. Phys.* **58** 4709–16

[23] Olsen R B and Brown D D 1982 High efficiency direct conversion of heat to electrical energy-related pyroelectric measurements *Ferroelectrics* **40** 17–27

[24] Kouchachvili L and Ikura M 2007 Pyroelectric conversion—effects of P(VDF–TrFE) preconditioning on power conversion *J. Electrostat.* **65** 182–8

[25] Rowe D M 1999 Thermoelectric, an environement-friendly source of electrical power *Renew. Energy* **16** 1251–6

[26] Chen M and Lu S-S 2005 On the figure of merit of thermoelectric generators *J. Energy Resources Technol.* **127** 37–41

[27] Niu X, Yu J and Wang S 2009 Experimental study on low-temperature waste heat thermoelectric generator *J. Power Sources* **188** 621–6

[28] Saqr K M, Mansour M K and Musa M N 2008 Thermal design of automobile exhaust based thermoelectric generators: objectives and challenges *Int. J. Automot. Technol.* **9** 155–60

[29] Yu J and Zhao H 2007 A numerical model for thermoelectric generator with the parallel-plate heat exchanger *J. Power Sources* **172** 428–34

[30] Wanga Z, Leonov V, Fiorini P and Van Hoof C 2009 Realization of a wearable miniaturized thermoelectric generator for human body applications *Sensors Actuators* A at press (doi:10.1016/j.sna.2009.02.028)

[31] Min G, Rowe D M and Kontostavlakis K 2004 Thermoelectric figure-of-merit under large temperature differences *J. Phys. D: Appl. Phys.* **37** 1301–4

[32] Cadoff I B and Miller E 1960 *Thermoelectric Materials and Devices* (New York: Reinhold Publishing Corporation)

[33] Beyer H, Nurnus J, Böttner H, Lambrecht A, Wagner E and Bauer G 2002 High thermoelectric figure of merit ZT in PbTe and Bi$_2$Te$_3$-based superlattices by a reduction of the thermal conductivity *Physica* E **13** 965–8

[34] Sklar A 2005 A numerical investigation of a thermodielectric power generation system *PhD Dissertation* Georgia Institute of Technology